is paper describes objective technical results and analysis. Any subjective views or opinions that might be express
the paper do not necessarily represent the views of the U.S. Department of Energy or the United States Governm

# Exploiting Model Structu SAND2019-7056C Propagation of Uncertainty in Earth System Models

Cosmin Safta

Sandia National Laboratories,
Livermore, CA, USA

joint work with
Alex Gorodetsky (UMich), John Jakeman, Khachik Sargsyan (SNL)
Daniel Ricciuto (ORNL)

Monday June 24 – UNCECOMP 19

oratories is a multimission laboratory managed and operated by National Technology & Engineering Solutions of Sandia,
neywell International Inc., for the U.S. Department of Energy's National Nuclear Security Administration under contract

# Acknowledgements


- This material is based upon work supported by the U.S. Department of Energy, Office of Science, Office of Advanced Scientific Computing Research (ASCR), Office of Biological and Environmental Research (BER), and Scientific Discovery through Advanced Computing (SciDAC) program.
- This study used resources of the Oak Ridge Leadership Computing Facility at the SAND2018-13880C Oak Ridge National Laboratory, which is supported by the Office of Science of the U.S. Department of Energy under Contract No. DE-AC05-00OR22725.
- Sandia National Laboratories is a multimission laboratory managed and operated by National Technology & Engineering Solutions of Sandia, LLC, a wholly owned subsidiary of Honeywell International Inc., for the U.S. Department of Energy's National Nuclear Security Administration under contract DE-NA0003525.

# Outline

1. Motivation/Model Problem
2. Low-Rank Functional Tensor-Train Approximation
3. Earth System Model Results

# E3SM Land Model (ELM)

- US Department of Energy (DOE) sponsored Earth system model
- Land, atmosphere, ocean, ice, human system components
- High-resolution, employ DOE leadership-class computing facilities
- Some of the results are with ELM-LF: a lower-fidelity, python version

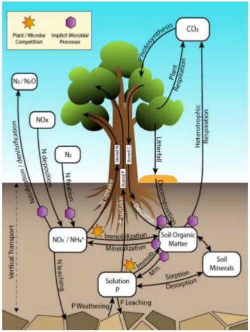


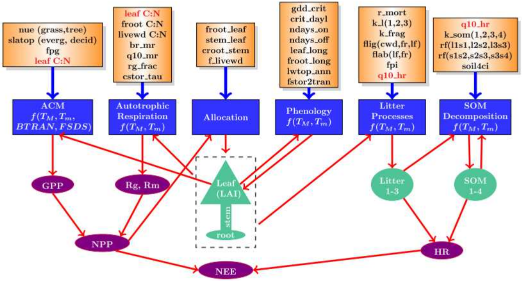

# ELM-LF: Model Workflow

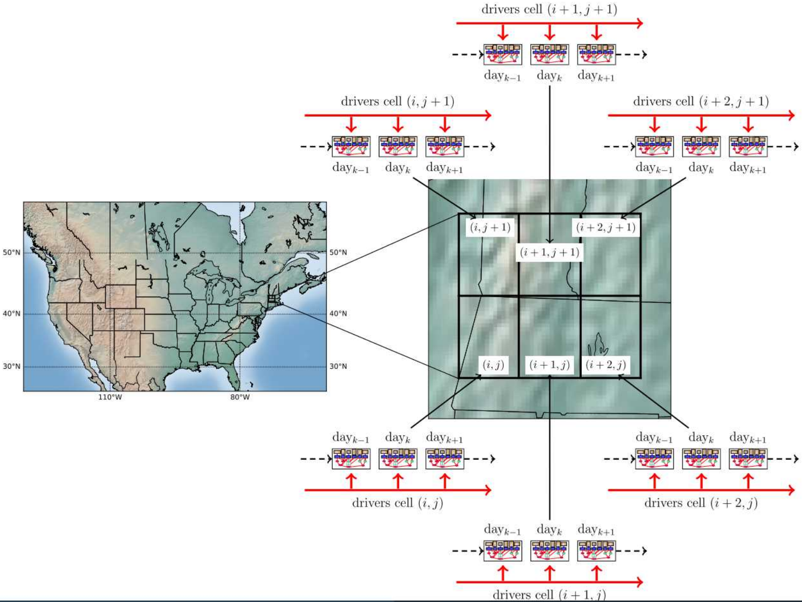

# ELM-LF: Pushed-forward Prior Distributions

- Uniform priors for all model parameters
    - bounds set based on physical constraints and/or information from subject matter experts

Harvard Forest EMS Tower (42.5° $N$,75.2° $W$)

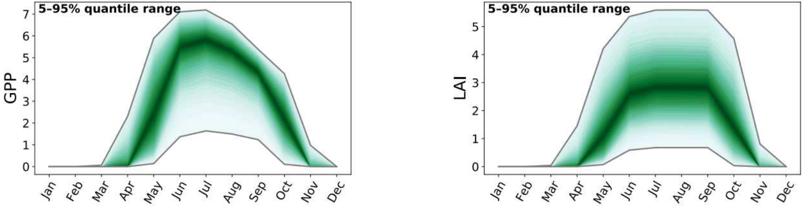


University of Michigan Biological Station (45.6° $N$,84.7° $W$)

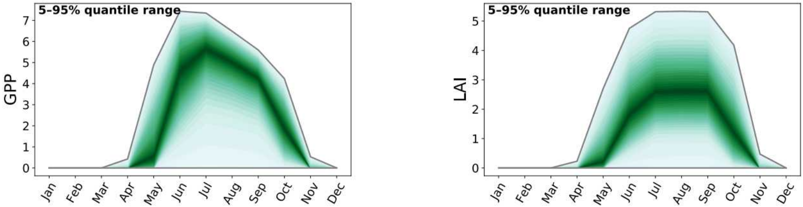

# ELM-LF: Sample Spatial Patterns

Gross Primary Production (GPP)

- spatio-temporal patterns for one parameter sample

April

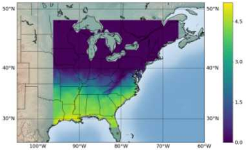

June

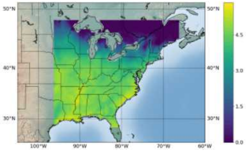

August

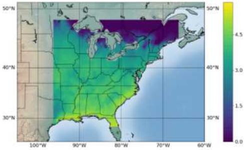

September

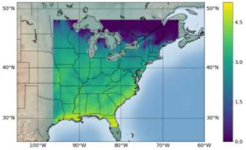

October

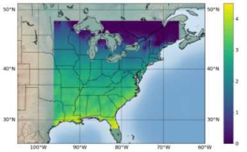

November

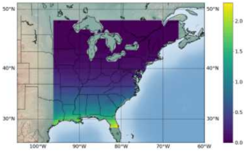

# Outline

1. Motivation/Model Problem
2. Low-Rank Functional Tensor-Train Approximation
3. Earth System Model Results

# Surrogates via Low-Rank Tensor Train Models

Tackle high-dimensionality and computational expense in Earth System Models via Global Sensitivity Analysis

- Explore Model Structure
- Seek efficient surrogate models for subsequent analysis of E3SM model components.

The low-rank functional tensor-train representation employs a set of matrix-valued functions in a tensor-train format to reveal couplings in high-dimensional models

- Subsequent Global Sensitivity Analysis results reveal that only a small number of parameters are driving the variability in output Quantities of Interest (QoIs).
- furthermore, spatial and temporal proximity results in correlated model behaviors.

# Low-Rank Tensor-Train

Employ an approach analoguous to low-rank tensor decompositions:

$$f(x_1, x_2, \ldots x_d) = \sum_{i_0=1}^{r_0} \sum_{i_1=1}^{r_1} \cdots \sum_{i_d=1}^{r_d} f_1^{(i_0 i_1)}(x_1) f_2^{(i_1 i_2)}(x_2) \cdots f_d^{(i_{d-1} i_d)}(x_d)$$

A compact expression can be assembled using a set of products of matrix-valued functions

$$f(x_1, x_2, \ldots x_d) = \mathcal{F}_1(x_1)\mathcal{F}_2(x_2) \cdots \mathcal{F}_d(x_d)$$

Each matrix-valued function $\mathcal{F}_k(x_k)$ is a collection of univariate functions

$$\mathcal{F}_i(x_i) = \begin{bmatrix} f_k^{(11)}(x_k) & f_k^{(12)}(x_k) & \ldots & f_k^{(1 r_k)}(x_k) \\ f_k^{(21)}(x_k) & f_k^{(22)}(x_k) & \ldots & f_k^{(2 r_k)}(x_k) \\ \vdots & \vdots & \ddots & \vdots \\ f_k^{(r_{i-1} 1)}(x_k) & f_k^{(r_{i-1} 2)}(x_k) & \ldots & f_k^{(r_{i-1} r_k)}(x_k) \end{bmatrix}$$

# Low-Rank Tensor-Train – Univariate Functions

The univariate function $f_k^{(ij)}(x_k)$ can be viewed as a random variable induced by the uniform random input $\xi_k$,

$$\xi_k \to x_k \to f_k^{(ij)}(x_k(\xi_k))$$

and can written as a Polynomial Chaos Expansion with respect to standard polynomials $\Psi_\alpha(\xi_k)$,

$$f_k^{(ij)}(x_k(\xi_k)) \approx \sum_{l=0}^{p_k} \theta_{ijkl} \Psi_l^{(ijk)}(\xi_k),$$

where $p_k$ is the number of basis terms chosen to approximate $f_k^{(ij)}(x_k(\xi_k))$.

- Legendre polynomials are orthogonal with respect to uniform measure of $\xi_k$, $\pi(\xi_k) = 1/2$ in $[-1, 1]$

$$\langle \Psi_\alpha(\xi_k)\Psi_{\alpha'}(\xi_k)\rangle \equiv \int_{-1}^{1} \Psi_\alpha(\xi_k)\Psi_{\alpha'}(\xi_k)\pi(\xi_k)d\xi_k = \delta_{\alpha\alpha'}\langle\Psi_\alpha(\xi_k)^2\rangle$$

- Other polynomials are available depending on the expected behavior of the QoIs.

# Low-Rank Tensor-Train – Optimization

- Consider a number of ELM-LF model results **y** corresponding to a set of choices **x** for the model inputs.

$$\mathrm{argmin}_{\boldsymbol{\theta}}||\boldsymbol{y}-\boldsymbol{f}||_2^2+\Omega[\boldsymbol{f}]$$

- A penalty term is added to minimize the norm of the functions in the matrix-valued $\mathcal{F}_k(x_k)$

$$\Omega[\boldsymbol{f}]=\lambda\sum_{k=1}^{d}\sum_{i=1}^{r_{k-1}}\sum_{j=1}^{r_k}||f_k^{ij}||^2$$

- Quasi-Newton method using L-BBFGS

C$^3$: Compressed Continuous Computation library
`https://github.com/goroda/Compressed-Continuous-Computation`

# Outline

1. Motivation/Model Problem
2. Low-Rank Functional Tensor-Train Approximation
3. Earth System Model Results

# Sequence of Tests

- Summary of Low-Rank Function Tensor Train (LRFTT) Approximation Model Fits
    - select polynomial orders (same for all univariate functions), TT rank, and regularization constant through cross-validation $\rightarrow$ explore a 3D grid of choices
- Comparison with Polynomial Chaos Models (PCE) via Sparse Regression
    - . . . via Bayesian Compressive Sensing
    - `https://www.sandia.gov/UQToolkit`
- 1000-2000 model simulations
    - (Randomized) Partioned into training and testing sets
    - K-fold cross-validation (4 folds)
- Global Sensitivity Sensitivity Analysis Results
    - ELM-LF monthly averages for select QoIs: LAI & GPP

# LRFTT Cross-validation: Ranks and Polynomial Orders

*Leaf Area Index (LAI)*

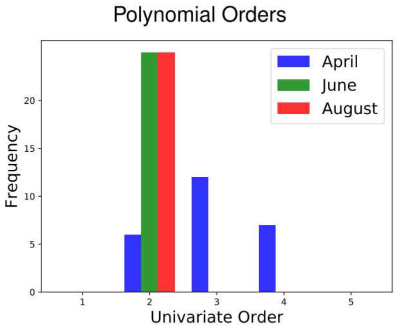


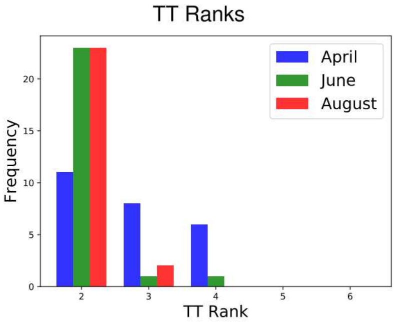

# LRFTT Cross-validation: Ranks and Polynomial Orders

## *Gross Primary Production (GPP)*

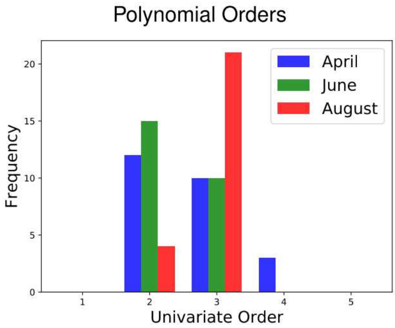


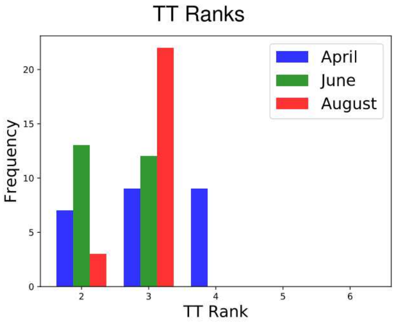

# LRFTT vs Sparse Polynomial Chaos Expansions

LRFTT: parameter ordering matters → explore several permutations

| Name | Sequence of processes |
|---|---|
| $lr_0$: | **acm, ar, alloc, phen, litter, decomp** |
| $lr_1$: | decomp, alloc, acm, ar, phen, litter |
| $lr_2$: | phen, decomp, ar, litter, alloc, acm |
| ... | ... |
| $lr_5$: | alloc, phen, ar, decomp, acm, litter |
| ... | ... |
| $lr_8$: | ar, alloc, decomp, litter, acm, phen |
| ... | ... |

Sparse PCE results denoted as *pce*

# GPP Accuracy: LRFTT vs Sparse PCE

April @ US-Ha1

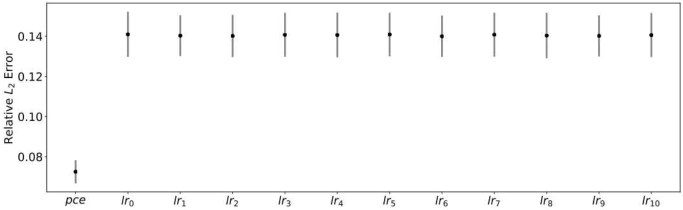


June @ US-Ha1

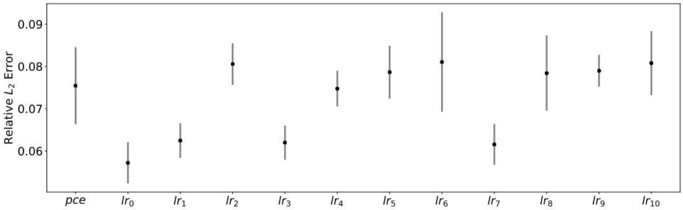

# LAI Accuracy: LRFTT vs Sparse PCE

April @ US-Ha1

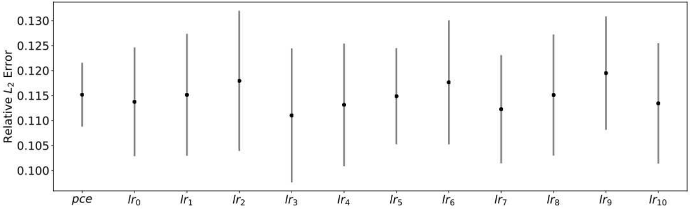


June @ US-Ha1

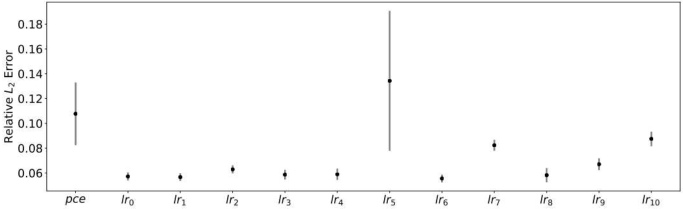

# LAI Accuracy: LRFTT vs Sparse PCE

June @ US-Ha1

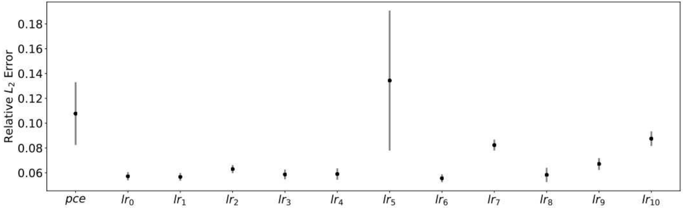


August @ US-Ha1

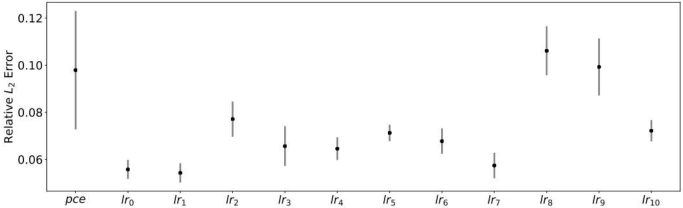

# GSA - Total Effect Sobol Indices

- Results corresponding to US-Ha1 site
- Sobol indices correspond to monthly QoI averages over 1980-2009
- Temporal trends match subject matter expert intuition for relevant processes controling GPP and LAI.

GPP

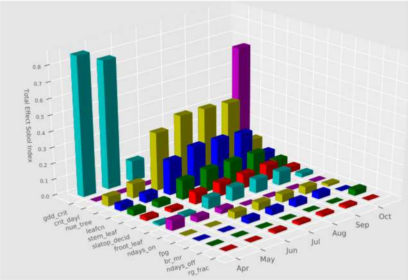


LAI

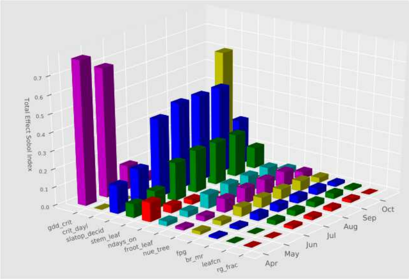

# Summary and Future Work

- Functional low-rank approximations proved efficient in capturing input-output dependencies imposed by land model processes.
    - Land Model is amenable to surrogate modeling via low-rank interactions.
    - For this set of models the low-rank functional approximation performs slightly better compared to a sparse regression polynomial chaos fit.
    - Identified a set of 10-12 parameters (out of 47) which are driving the variance in the selected QoIs.
- Exploring techniques for discovering and folding spatial dependencies (space/time) into the low-rank approximation.